3D THERMOGRAPHY FOR QUANTIFICATION OF HEAT GENERATION RESULTING FROM INFLAMMATION

THERMOGRAPHIE 3D POUR LA QUANTIFICATION DE LA CHALEUR PRODUITE PAR UNE INFLAMMATION

Abstract

We aim to develop a non-invasive imaging technology to allow early, accurate and quantitative detection of inflammation. Thermography has been used for decades by biologists and clinicians to isolate main sites of body heat loss and to assist with diagnosis of biomechanical problems. However, thermography is still viewed as an accessory to conventional clinical examination procedures because it only provides qualitative data. The new technology we develop will greatly enhance the usefulness of thermography for clinicians, as it will provide quantifiable data. This technology is based on the combination of visual 3D imaging technology and thermal imaging technology. The combination of these imaging facilities allows the generation of combined 3D and thermal data from which thermal signatures can be quantified.

Résumé

Nous visons à développer une technologie non envahissante permettant la détection préventive d'inflammations de façon précise et quantitative. La thermographie est employée depuis des décennies par des biologistes et des cliniciens pour déterminer les lieux principaux de pertes de chaleur et pour assister le diagnostique de certains problèmes biomécaniques. Cependant, la thermographie est encore regardée comme un gadget face aux procédures cliniques conventionnelles parce qu'elle ne fournit que des données qualitatives. La nouvelle technologie que nous développons augmentera considérablement l'utilité de la thermographie pour les cliniciens, car elle fournira des données quantifiables. Cette technologie est basée sur la combinaison d'un scanner 3D et d'un appareil photo thermique. La combinaison de ces technologies permet la génération d'images 3D combinées avec des données thermiques à partir desquels des signatures thermiques peuvent être mesurées.

Jean-Christophe Nebel
Computer Vision and Graphics,
Department of Computing Science,
University of Glasgow,
17 Lilybank Gardens, G12 8QQ,
Glasgow, Scotland, UK
Tel: +44 (0)141 330 6813
Fax: +44 (0)141 330 3119
jc@dcs.gla.ac.uk

3D thermography for quantification of heat generation resulting from inflammation

Pavel Aksenov, Iain Clark, David Grant,
Alan Inman, Leor Vartikovski and Jean-Christophe Nebel
Computer Vision and Graphics,
Department of Computing Science,
University of Glasgow,
17 Lilybank Gardens, G12 8QQ,
Glasgow, Scotland, UK
jc@dcs.gla.ac.uk

1. Introduction

We aim to develop a non-invasive imaging technology to allow early, accurate and quantitative detection of inflammation. Thermography has been used for decades by biologists and clinicians to isolate main sites of body heat loss and to assist with diagnosis of biomechanical problems. However, thermography is still viewed as an accessory to conventional clinical examination procedures because it only provides qualitative data. The new technology we develop will greatly enhance the usefulness of thermography for clinicians, as it will provide quantifiable data.

After having motivated our research, we present the configuration of the system we built. Finally we present some early results showing the process of thermogram quantification and its use for monitoring inflammations.

2. Motivation

All objects with a temperature above absolute zero emit infrared radiation from their surface. The Stefan-Boltzmann Law defines the relation between radiated energy and temperature by stating that the total radiation emitted by an object is directly proportional to the object's area and emissivity and the fourth power of its absolute temperature. Since the emissivity of human skin is extremely high (within 1% of that of a black body), measurements of infrared radiation emitted by the skin can be converted directly into accurate temperature values. This process is known as infrared thermography.

For nearly half a century research has been conducted on humans [La56] and animals [St74] showing the correlation between heat patterns and medical conditions (see Fig1.). In particular extensive research has studied skin surface temperature associated with breast cancer. In 1963, Lawson and Chughtai published a study demonstrating that the increase in regional skin surface temperature associated with breast cancer was related to both increased vascular flow and increased metabolism [La63]. In 1982, thermography was approved by the U.S. Food and Drug Administration (FDA) as a supplement to mammography in helping to detect breast cancer.
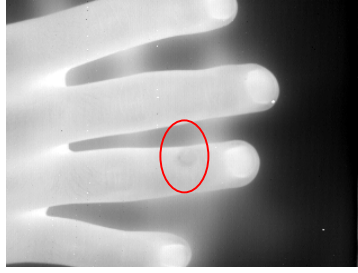
Figure 1: A wart displays abnormal thermal properties

Though thermography is FDA approved, this procedure, which is cheap and non-invasive - no radiation or intravenous injection is used – (examinations could be performed as often as indicated), has *not* gained acceptance in the medical and veterinary communities as a necessary or effective tool in inflammation and tumour detection. That can be explained by the fact that, so far, thermography has only provided qualitative data. Indeed, heat flux measured by an infrared camera depends on the distance and the orientation between the camera and the surface of the biological subject that is measured. Therefore a 2D thermograph can only provide qualitative data.

We propose to combine 3D surface models with 2D thermal images to enable us to measure quantitatively the heat flux emitted from the surface of a subject. Measuring the 3D surface enables us to compute the orientation and distance and between the camera and the surface of the subject hence allows us to quantify the actual heat flux emitted per unit surface area. A second advantage of this combination is that 3D thermographs can be easily registered which allows their comparison.

3. Data capture and 3D model generation

3.1 Principle

A 3D thermogram scanner is a piece of technology that has the capability of capturing 3D and infrared data in a synchronised manner: it does combine a 3D scanner and a thermal camera. Its configuration is shown on Figure 2.

Figure 2: Configuration of the3D thermogram scanner

The process of 3D capture relies upon stereo photogrammetry [Si00]: 2 high-resolution colour cameras generate colour images that are used for stereo range finding. And the infrared image is used to capture the thermal signature of the subject.

3.2 Hardware

3.2.1 Stereo pair of colour cameras

We use 2 high-resolution colour cameras, which are commercially available: Mamiya RZ67 PRO II, 6x7 cm SLR camera series connected to Kodak Professional DCS Pro Backs. Inside these ProBacks, there is a 16 megapixel sensor (4080x4080) generating a 48MB file. Moreover a capture software was written using the ProBack SDK in order to synchronise the capture of the stereo pair of cameras.

Figure 3: Colour camera used in the stereo pair

3.2.2 Thermal camera

Our thermal imager is an Indigo Systems Merlin Mid Camera. It uses cooled Indium Antimonide to detect infrared radiation in the 3-5μm waveband. The camera uses a GaAs based lens in order to capture the infrared radiation, as it will not penetrate through glass. The sensitivity of 25mK associated with the detector is necessary for detailed medical observation and quantification of heat flux. Moreover the response time of such detectors is in milliseconds, which allows the capture of real-time thermal signatures.

Figure 4: Thermal camera

3.3 3D Data generation

In order to build 3D models from the data captured by the scanner previously described, the cameras have to be calibrated, e.g. the detailed geometric configuration of all the cameras has to be known. Figure 5 shows a heated calibration target seen by the colour cameras and by the infrared camera. Then once the capture has been done, the stereo matching process is applied to the stereo-pair images. The algorithm we use is based on multi-resolution image correlation [Zh88].
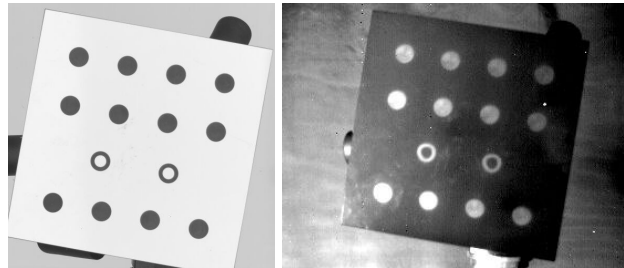

Figure 5: Calibration target seen by a colour and an infrared camera

Once the stereo matching process is completed, the final displacement files combined with the calibration file of the associated pod allow the generation of a range map, i.e. the map of the distances between each pixel and the coordinate system of the pod. An implicit surface is computed that merges together the point clouds into a single triangulated polygon mesh using a variant of the marching cubes algorithm [Lo87]. This mesh is then further decimated to any arbitrary lower resolution for display purposes.

The generation of a 3D thermogram is achieved by mapping the infrared picture taken by the infrared camera to the 3D geometry. Since the thermal camera and the stereo pair of cameras are calibrated together the mapping phase is quite straightforward. On Fig. 6, views of a 3D thermogram are shown.
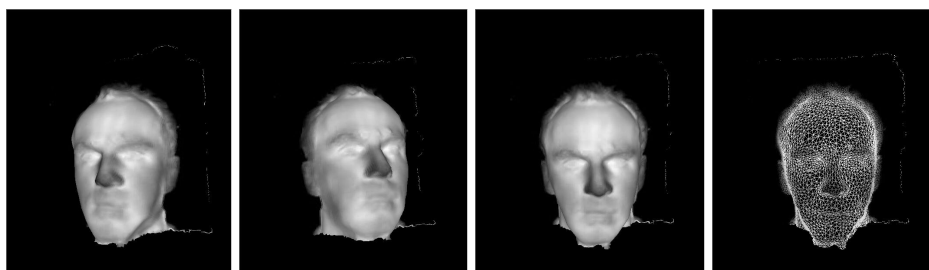

Figure 6: Views of a 3D thermogram

A more detailed presentation of the 3D capture system based on high-resolution colour cameras is given by Ju [Ju03].

3. Quantification of heat generation resulting from inflammation

3.1 Towards standardisation of thermograms

Since the heat flow measured by an infrared camera depends on the distance and the angle between the camera and the object of interest, observations depend on the position of the observer. Using the information of these 3D thermograms, we will be able to generate standardised thermograms, independent from camera position, which could be used for quantitative studies. These view independent thermal images generated from experimental data can then be subtracted from each other to monitor sequential evolution of an inflammatory pattern in terms of change in temperature and volume of inflamed tissue.

The flux, F in watt, is the instantaneous measure of the quantity of radiation. It describes the output of a source propagating in the form of a beam or received by a detector [Ga94]. If the radiance, L, is uniform, the flux is defined by

$$F = LG$$

where G is the geometrical spread of a beam.

The geometrical spread is given by

$$G = (SR \cos\Phi_1 . \cos\Phi_2)/d^2$$

where Φ_1 and Φ_2 are the angle between the line joining the source area, S, to the receptor area, R, and the normals N_S and N_R to S and R, respectively (see Fig. 7). And d is the distance between S and R.
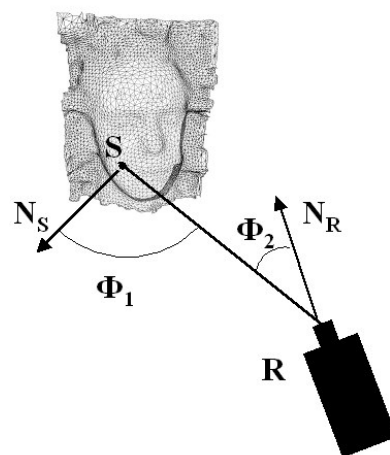

Figure 7: Flux measured by the thermal camera

Therefore, the flux becomes

$$F = LSR(cos\Phi_1.cos\Phi_2)/d^2$$

The flux measured by the thermal camera depends on the angle and distance between the object and the camera. In order to generate thermograms that are view independent, we offer to calculate a standardised flux, F_S, that we define as the quantity of radiation a thermal camera would measure while facing the source area at a distance of 1m

$$F_S = LSR = F. d^2/(cos\Phi_1.cos\Phi_2)$$

Fig. 8 shows a thermogram and its corresponding distance and angle maps generated using the 3D information provided by the 3D model.

Figure 8: Thermogram, distance and angle maps

Fig. 9 shows a raw thermogram and the generated standardised thermogram based on the assumption that pixel values are proportional to flux values. It can be noticed that areas with normals pointing away from the camera (white areas on the angle map) are much brighter on the standardised thermogram than on the raw thermogram.

Figure 9: Original and standardised thermogram

We are currently designing radiometric calibration procedures for quantification of temperature from thermal flux data: capture of visual and thermal illumination of geometric models with simultaneous direct measurement of surface temperatures, using copper-constantine thermocouples. This process will provide the necessary data from which view independent temperature data can be calculated.

3.2 Thermogram registration

Another advantage of dealing with 3D thermograms is that thermograms can be registered accurately using registration algorithms based on 3D surface shapes. Our registration process is based on the Iterative Closest Point algorithm (ICP) [Be92]. It establishes correspondences between data sets by matching points in one data set to the closest points in the other data set. It is an iterative process going through the following steps:

- For each point of mesh A, compute the closest point of mesh B.
- Solving a minimization problem, compute the registration vector.
- Apply the registration and update the position of the points of mesh B.
- Compute the mean square error of the previous iteration and the current iteration.
- Terminate the iteration if the change in mean square error is less than a preset threshold.

ICP is a very powerful algorithm; in particular it can handle a reasonable amount of noise. However since it is an iteration of minimisation problem, the algorithm may converge towards a local minimum. Generally it is overcome by starting the iteration loop from an approximate registration. Since we usually wish to compare similar areas captured in similar conditions, the generated 3D thermograms are already approximately registered, which is generally sufficient for getting the ICP algorithm to converge without manual intervention. However if these conditions cannot be fulfilled, the registration process is then done in two steps. The first step normalises the position of the 3D thermograms data using a Procrustes registration. The second one refines the registration using the ICP algorithm.

Figure 10: Set of thermograms

The registration of 3D thermograms allows the projection of their textures in any plane that can then be used for their comparison (see Fig. 10 and 11).
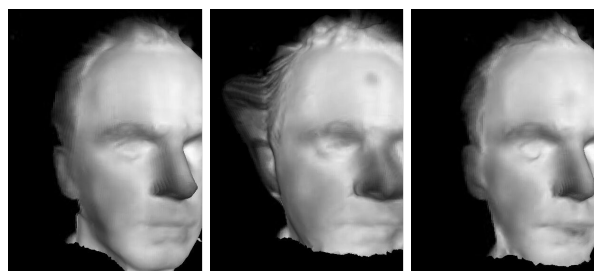

Figure 11: Same set of registered thermograms

3.3 Thermogram comparison

Once thermograms are registered, any image processing technique can be used for their analysis. We have started to investigate the automatic detection, monitoring and quantification of inflammations. The idea is either to compare longitudinally thermographs of the same area in order to monitor the healing of an inflammation or to detect and quantify an inflammation by comparing the thermogram of interest either with a symmetrical area or with a normal thermogram.

Figure 12: Registered, substracted and thresholded thermograms

The first task is to subtract images to keep only areas where thermal signatures are different. On Fig. 12, a cold spot was added on the brow of the second model. Then these subtracted images are processed to detect areas of interest on thermographs. We use operators of binary morphology [Ha87] and [Mo00] after having converted the subtracted images into binary images by thresholding.

The first phase of the processing requires filtering off the camera noise. That is performed by an erosion process that removes each object pixel not having a given neighbourhood in its background. Then a dilation process is applied: that expands each object pixel with the given neighbourhood, which, practically, reconstruct the previously eroded bigger objects. These 2 successive operations are called an opening and allow discarding object of small sizes.
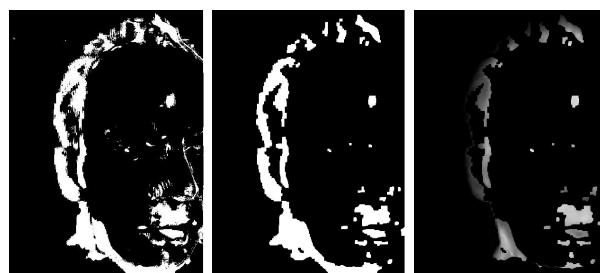

Figure 13: Thresholded, filtered and masked thermograms

The second phase is called a closing. It consists of a number of dilations followed by the same number of erosions. That allows the connection of disconnected object parts, the closing of holes and the smoothing of contours. The result of this phase is a set of continuous areas that represent areas of inflammation. These areas can be then used as a mask on the grey levels thermographs, so that regions of interest are kept (see Fig. 13). Further processing would be needed to filter out areas that are not of interest.

Then for each selected area further analysis can be performed such as size computation, calculation of the amount of generated energy or the gradient of energy. Finally comparison between this data collected from different thermograms can be made to allow the detection or the monitoring of an inflammatory condition.

On Fig. 14, we compare the knees of an athlete who has a knee inflammation. The original 3D thermogram was cut in two to generate a mesh for each knee. Then the mesh of the left knee was mirrored and registered with the mesh of the right knee. After processing, the inflamed area is clearly visible on the masked thermogram.
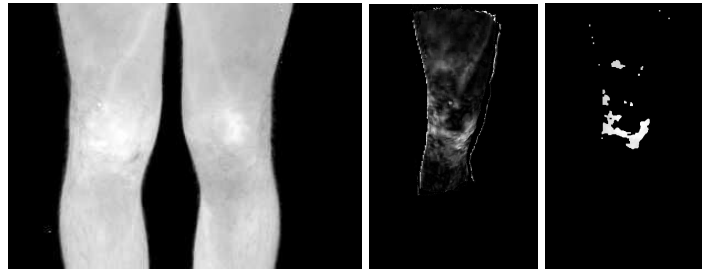

Figure 14: Original, substracted and masked thermograms

4. Conclusion

We presented in this paper a new type of 3D scanners: a 3D scanner that has the capability of generating 3D thermograms. We detailed the process of thermogram quantification and showed some early results. Finally we demonstrated that since 3D thermograms can be registered accurately, comparisons and analyses can be performed using standard image processing techniques: results on face and knee thermographs show that cold or inflamed areas can be detected easily.

We have started a more in-depth investigation of the generation of standardised thermograms by designing radiometric calibration procedures based on copper-constantine thermocouple measurements. Moreover we expect to start shortly a pilot study with clinicians who will be able to assess and guide our work regarding the early, accurate and quantitative detection of inflammation.

5 References

[Ar87] *K.S. Arun, T.S. Huang, and S.D. Blostein*. "Least-square fitting of two 3d point sets". *IEEE Trans. Pattern Anal. Machine Intell.*, 9(5):698-700, September 1987.
[Be92] *P. J. Besl and N. D. McKay*, "A Method of Registration of 3-D Shapes", *IEEE Trans. Pattern Analysis and Machine Intelligence*, vol. 14, no. 2, pp. 239 - 255, Feb. 1992.
[Ga94] *G. Gaussorgues*, Infrared Thermography, Microwave Technology Series 5, Chapman and Hall, London, 1994.
[Ha87] *R. M. Haralick, S. R. Sternberg and X. Zhuang*, Image Algebra Using Mathematical Morphology, IEEE Trans. PAMI, vol. 9, pp. 532-550, July 1987.
[Ju03] *X. Ju, P. Siebert*, High resolution stereo system, Proc. 3D Modelling 2003, Paris, France, 2003
[La56] *R. Lawson,* Implications of Surface Temperatures in the Diagnosis of Breast Cancer. Can Med Assoc J 75: 309-310,1956.

[La63] *R. Lawson and M. S. Chughtai*, Breast cancer and body temperatures. Can Med Assoc J 88: 68-70,1963.

[Lo87] *W. E. Lorensen and H.e Cline*, Marching cubes: a high resolution 3D surface construction algorithm, ACM Computer Graphics, 21, 1987

[Mo00] *B. S. Morse*, Lecture note: Binary Morphology, Young University, 2000, rivit.cs.byu.edu/550/W02/lectures/lect05/morph1.pdf

[Si00] *J. P. Siebert and S. J. Marshall*, Human body 3D imaging by speckle texture projection photogrammetry, Sensor Review 20 (3), p.p. 218-226, 2000.

[Sm02] *S. T. Smith*, Modelling Hot Bodies: Combined real-time 3D and Thermal Imaging for Medical Applications, Information Technology, MSc IT project report, Glasgow Univ., 2002.

[St74] B. *Stromberg,* The use of thermography in equine orthopedics. J Vet Radiol 1974.

[Tu01] *T. A. Turner,* Diagnositc thermography. *Veterinary Clinics of North America. Equine Practice*. 17(1): 95 – 112, 2001.

[Zh88] *J. Zhengping*, On the multi-scale iconic representation for low-level computer vision systems. PhD thesis, The Turing Institute and The University of Strathclyde, 1988.